

The Stellar Merger Scenario for Black Holes in the Pair-instability Gap

M. RENZO,^{1,2} M. CANTIELLO,^{1,3} B. D. METZGER,^{2,1} AND Y.-F. JIANG (姜燕飞)¹

¹*Center for Computational Astrophysics, Flatiron Institute, New York, NY 10010, USA*

²*Department of Physics, Columbia University, New York, NY 10027, USA*

³*Department of Astrophysical Sciences, Princeton University, Princeton, NJ 08544, USA*

ABSTRACT

The recent detection of GW190521 stimulated ideas on how to populate the predicted black hole (BH) pair-instability mass gap. One proposal is the dynamical merger of two stars below the pair instability regime forming a star with a small core and an over-sized envelope. We outline the main challenges this scenario faces to form one BH in the gap. In particular, the core needs to avoid growing during the merger, and the merger product needs to retain enough mass, including in the subsequent evolution, and at core-collapse. We explore this scenario with detailed stellar evolution calculations, starting with ad-hoc initial conditions enforcing no core growth during the merger. We find that these massive merger products are likely helium-rich and spend most of their remaining lifetime within regions of instabilities in the Hertzsprung-Russell diagram, such as luminous blue variable eruptions. An energetic estimate of the amount of mass loss neglecting the back-reaction of the star suggests that the total amount of mass that can be removed at low metallicity is $\lesssim 1 M_{\odot}$. This is small enough that at core-collapse our models are retaining sufficient mass to form black holes in the pair-instability gap similar to the recent ones detected by LIGO/Virgo. However, mass loss at the time of merger, the resulting core structure, and the mass loss at core collapse still need to be quantified for these models to confirm the viability of this scenario.

Keywords: stars: black holes – stars: massive – stars: LBV – stars: merger

1. INTRODUCTION

The existence of a mass gap where pair-instability (PI) supernovae (SNe, e.g. Barkat et al. 1967) prevent the formation of black holes (BH) is a robust prediction of stellar evolution theory (e.g., Woosley et al. 2002; Woosley 2017; Marchant et al. 2019; Farmer et al. 2019; Leung et al. 2019; Renzo et al. 2020b,a; Marchant & Moriya 2020). However, the detection GW190521 (Abbott et al. 2020a,b) is challenging this prediction. For this merger event *both* BH masses¹, $85_{-14}^{+21} M_{\odot}$ and $66_{-18}^{+17} M_{\odot}$, are in the PI mass gap situated roughly between $\sim 45 M_{\odot}$ and $\sim 130 M_{\odot}$ (e.g., Woosley et al. 2002; Farmer et al. 2019, 2020).

These BHs might not be the direct remnants of stars, but rather the product of second-generation BH mergers in a (nuclear) cluster (e.g., Perna et al. 2019; Rodriguez et al. 2020; Mapelli et al. 2020; Kremer et al. 2020; Fragione et al. 2020) or AGN disk (e.g., McKernan et al. 2012, 2014; Bartos et al. 2017; Stone et al. 2017; Fra-

gione et al. 2019), of accretion from gas clouds (e.g., Roupas & Kazanas 2019; Safarzadeh & Haiman 2020), or possibly primordial BHs (De Luca et al. 2020).

Many possible stellar explanations for the formation of BHs in the gap have also been proposed. These include: reduction by $\gtrsim 2\sigma$ of the $^{12}\text{C}(\alpha, \gamma)^{16}\text{O}$ reaction rate (Farmer et al. 2020; Belczynski 2020), modifications to the standard model (Croon et al. 2020a,b; Sakstein et al. 2020), and population III stars (Farrell et al. 2020; Kinugawa et al. 2020). BHs accreting in isolated binaries do not contribute significantly to populating the pair-instability mass gap (van Son et al. 2020).

We focus on one particular scenario proposed by Spera et al. (2019); Di Carlo et al. (2019, 2020a,b): the formation of BHs in the PI mass gap via stellar mergers in a dynamical environment. Sec. 2 summarizes this “stellar merger” scenario and its challenges. We then construct stellar models for the merger product in Sec. 3 and evolve them. Sec. 4 shows how evolutionary processes can lead to continuum-driven mass-loss which is not considered in rapid population-synthesis models underlying N-body calculations. We estimate the amount of mass loss, and conclude that by itself it might not change the scenario appreciably.

¹ However, see also Fishbach & Holz (2020) for a population-informed re-analysis reconciling the masses with stellar evolution predictions.

2. THE STELLAR MERGER SCENARIO

Di Carlo et al. (2020b) present a detailed example of this scenario (see their Fig. 7), where the dynamically-driven merger happens at the end of the main sequence of a $\sim 58 M_{\odot}$ star. At this point the total mass of a $\sim 42 M_{\odot}$ star is added to the envelope *without* modifying the core. Thus, the merger product has a small core and an over-sized envelope, and reaches core-collapse (CC) with a total mass of $\sim 99 M_{\odot}$. At this point, Di Carlo et al. (2019, 2020a,b) assume a direct collapse to BH, without mass ejection but accounting for a reduction in gravitational mass due to neutrino losses.

In order to form a coalescing binary BH with masses in the PI mass gap, this scenario faces the following four challenges.

2.1. *The merger challenge: mass loss, core size, and rotation*

The first challenge is retaining sufficient mass during the stellar collision and forming a post-merger structure without modifying the core.

Lombardi et al. (2002) performed SPH simulations of low-mass stellar collisions and found their models lose 1–7% of the total mass during the mergers. Glebbeek et al. (2013) computed SPH simulations of head-on collisions of massive stars. For their most massive objects ($40 M_{\odot} + 40 M_{\odot}$) they found a mass loss corresponding to 6–8% of the total mass. However, these models neglect the effects of radiation transport, which could have an important role for the mass budget in the merger of very luminous stars. Including radiation effects would likely increase the mass-loss rate during the merger, because the radiation-pressure dominated envelope of very massive stars are loosely bound and easily stripped.

A back-of-the-envelope estimate of the amount of mass loss can be obtained considering the energy available to drive mass loss is (a fraction of) the relative kinetic energy of the two incoming stars

$$E_{\text{kin}} \sim \frac{1}{2} \frac{M_1 M_2}{M_1 + M_2} v_{\sigma}^2 \lesssim 10^{46} \text{ erg} \ll E_{\text{bind}} \quad , \quad (1)$$

where we use the aforementioned masses and assume $v_{\sigma} \lesssim 10 \text{ km s}^{-1}$ as the velocity dispersion of the cluster, and E_{bind} is the typical binding energy of the stars. Our pre-merger models (see Sec. 3) only have $\lesssim 10^{-3} M_{\odot}$ with binding energy lower than 10^{46} erg . This suggests that mergers resulting in small mass loss might be possible, however, using instead the escape velocity from the star in E_{kin} would result in a significantly higher mass loss. Our estimate neglects the stellar reaction to the energy injection during the merger process.

A second challenge is maintaining the core mass below the pulsational pair-instability (PPI) regime. The result

of a stellar collision is often approximated using entropy sorting (e.g., Lombardi et al. 2002; Gaburov et al. 2008): this would effectively result in merging the cores of both stars and increasing the resulting core mass. Dynamical interaction might also pair stars in tight binaries merging later in a common envelope event. Merger simulations involving one evolved and one unevolved star are often invoked to explain the progenitor of SN1987A (e.g., Podsiadlowski 1992; Menon & Heger 2017), and in this case mixing into the core decreasing its mass has been proposed.

Mergers products are also expected to be fast rotators (e.g., de Mink et al. 2013), although Schneider et al. (2019) found internal redistribution of angular momentum preventing fast surface rotation. If a large amount of angular momentum is transported in the core, rotational mixing (e.g., Maeder & Meynet 2000) might increase the core mass pushing the star into the PPI regime.

We do not investigate how realistic is the merger structure proposed by Spera et al. (2019); Di Carlo et al. (2020a,b). Following these studies, we assume no mass is lost during the merger process and we do not consider the effects of rotation.

2.2. *The evolution challenge: winds and envelope instabilities*

After the merger, low metallicity is necessary to prevent large line-driven wind mass loss (e.g., Farrell et al. 2020; Kinugawa et al. 2020), or these have to be artificially suppressed (Belczynski et al. 2020). The angular momentum distribution might also lead to centrifugally-driven mass loss (Langer 1998; Heger et al. 2000; Zhao & Fuller 2020).

Other modes of mass loss such as continuum-driven winds and/or luminous blue variable (LBV) eruptions are typically not considered. However, merger products are prime candidates to explain LBV stars (e.g., Justham et al. 2014; Aghakhanloo et al. 2017) because of their increased luminosity, non-standard internal structure, and possible He-enrichment. He opacity is thought to have a key role in driving eruptive mass loss (Jiang et al. 2018), which could make this type of mass loss relatively metallicity-independent.

Our simple models presented in Sec. 4 address mainly this problem at metallicity $Z = 2 \times 10^{-4}$ (e.g., Di Carlo et al. 2020a), however this challenge is expected to become progressively harder at higher Z , because of the increasing opacity in the stellar envelope.

2.3. The collapse challenge: mass loss at black hole formation

At BH formation, $\sim 10^{53}$ erg of neutrino emission is expected to suddenly decrease the gravitational mass of the collapsing core. This in turn creates a shock propagating through the envelope that can unbind the outer-layers (e.g., Nadezhin 1980; Lovegrove & Woosley 2013; Fernández et al. 2018). While in the calculations of Di Carlo et al. (2020b) the BH mass accounts for the neutrino losses, the impact on the envelope mass loss was not investigated.

If the envelope is not lost at core collapse, it still could retain enough angular momentum to allow for the formation of an accretion disk. This could result in (ultra)-long gamma-ray bursts (e.g., Perna et al. 2018) and the delayed ejection of a significant fraction of the envelope. Even in the absence of net rotation, the fallback of large convective cells in the envelope could also drive the formation of disks and ultimately produce large amounts of mass loss through jets (Quataert et al. 2019).

2.4. The gravitational-wave challenge: dynamical pairing

If the previous challenges can be overcome, this scenario allows for the formation of single BHs in the gap. Dynamical interactions are then required to pair two of these BHs together in a tight orbit. Because of their large masses, these BHs are efficient at finding companions to merge with, with typical delay-time distribution of order tens of Myrs. Di Carlo et al. (2020a) finds a significant fraction of the merger rate from cluster dynamics to involve one BH from the stellar merger scenario (see also Spera et al. 2019; Di Carlo et al. 2019; Kremer et al. 2020; Di Carlo et al. 2020b). However, to explain the masses in GW190521, both BHs should have formed via such evolutionary path.

3. CONSTRUCTING A MERGER MODEL

We use Modules for Experiments in Stellar Astrophysics (MESA revision 12778, Paxton et al. 2011, 2013, 2015, 2018, 2019) to construct a post-merger structure. We do not compute the dynamical phase of the merger, but rather construct an ad-hoc post-merger structure starting from the pre-merger stars. Details of the numerical implementation, together with the microphysics inputs are given in Appendix A.

3.1. Initial chemical composition

Following Di Carlo et al. (2020b), we assume the merger happens at the end of the main sequence of a $M_1 = 58 M_\odot$ star at $Z = 2 \times 10^{-4}$. Using Brott et al. (2011) overshooting, its main-sequence lifetime is

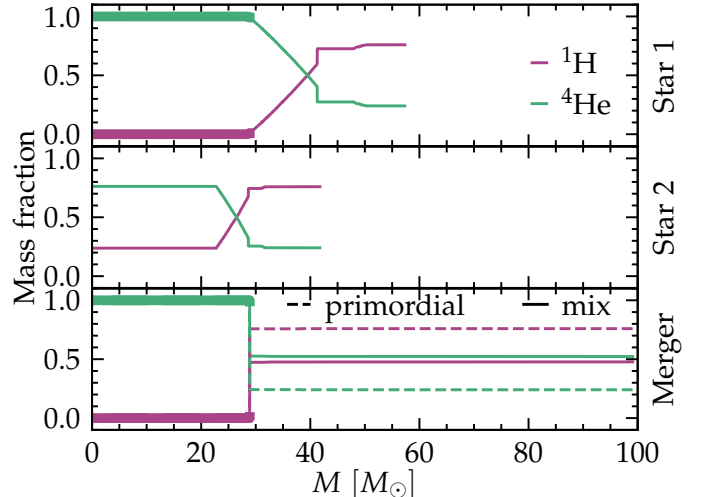


Figure 1. H and He profiles of the two pre-merger stars (top and middle panel) and of the merger products (bottom panel). In the bottom panel, solid (dashed) lines indicate the envelope composition for the “mix” (“primordial”) model. Both models have by construction the same core structure of the most massive star pre-merger (thicker lines). The least massive star 2 is too young to have a well defined He core.

$\tau_{\text{MS}} = 4.15$ Myr, and the corresponding Helium (He) core mass is $\sim 29 M_\odot$. This value is below the limit for any kind of PI pulse (Renzo et al. 2020a). We evolve up to τ_{MS} a $M_2 = 42 M_\odot$ star with the same setup. Very massive stars have comparable lifetimes, and by this time, the second star has a central He abundance $X_c(^4\text{He}) = 0.76$ extending out to mass coordinate $\sim 25 M_\odot$ (cf. middle panel of Fig. 1). The Kelvin-Helmholtz timescale of these stars is of order 10^4 years. After the merger, a relaxation phase of comparable duration is expected (although both the luminosity and radius are likely to be higher right after the merger, e.g., Schneider et al. 2019).

To construct the merger product, we first relax (e.g., Morozova et al. 2015; Vigna-Gómez et al. 2019) the most massive star model to $M_{\text{tot}} = M_1 + M_2 - \Delta M_{\text{wind}}$, where the mass lost to winds ΔM_{wind} is only $\sim 0.9 M_\odot$ using Vink et al. (2001) algorithm. The mass relaxation procedure does not account for the release of gravitational or internal energy from the newly accreted mass. Then, we relax the chemical composition of the merger.

The top two panels in Fig. 1 show the pre-merger composition of the two stars, and the bottom panel shows two different merger products. For both, we enforce the hypothesis of the “stellar merger scenario” maintaining the same composition and mass of the core of the most massive star (thick lines in Fig. 1).

The fact the second star has already synthesized a large amount of ^4He forces to make choices for the enve-

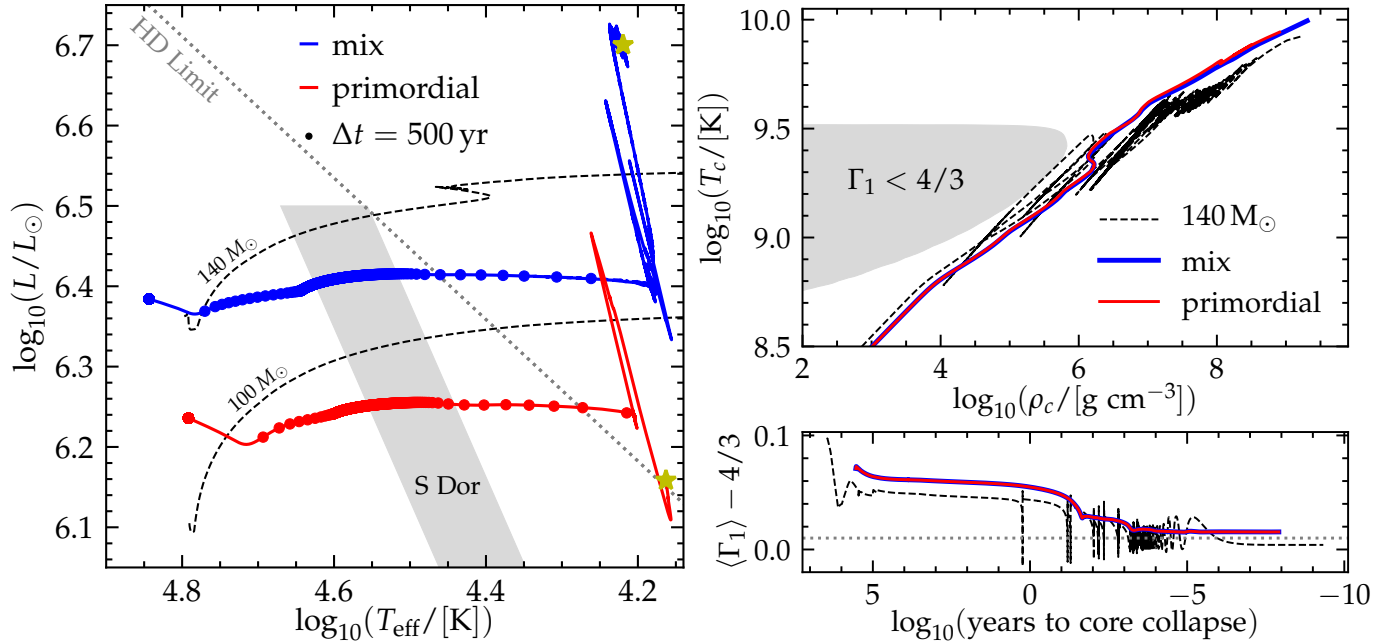


Figure 2. Left panel: HR diagram of the post-merger evolution. Each dot is separated by 500 years. The dashed black lines shows for comparison a H-rich $140 M_{\odot}$ star from Renzo et al. 2020a (smaller overshooting, encounters the PPI later), and a $100 M_{\odot}$ model (same overshooting, expected to encounter the PPI). The yellow stars mark the onset of core collapse. Top right panel: evolution of the central temperature and density. Bottom right panel: time evolution of the pressure-weighted average adiabatic index, the star becomes pair-unstable when it drops below the dotted horizontal line (Renzo et al. 2020a).

lope composition. Usually, mergers are built assuming that the lowest entropy layers sink to the bottom. However, this would result in a larger He core mass, entering the PPI regime, and violating the hypothesis of the scenario. Instead, in model “mix” (solid lines in the bottom panel of Fig. 1) we fully mix the envelope of the most massive star with the entire second star at merger time. This represents the most favorable scenario preventing growth of the He core, leading to the formation of a He-rich envelope with $X(^4\text{He}) \simeq 0.52$. The total mass in each element is conserved to better than 2%.

As the opposite limiting case, in model “primordial” (dashed lines in the bottom panel Fig. 1) we ignore the composition of the second star, and increase the envelope mass with the initial composition, that is with a He abundance of $X(^4\text{He}) \simeq 0.24$. This corresponds to a merger between an evolved primary and a newly formed secondary star with its primordial chemical composition.

4. POST-MERGER EVOLUTION

We evolve our merger models until the onset of CC. The left panel of Fig. 2 shows their post-merger Hertzsprung-Russell (HR) diagram. The evolution proceeds from left towards cooler temperatures. The more He-rich “mix” model has a higher luminosity (L). This can be understood considering that $L \propto \mu^4$ where μ is the mean molecular weight for an ideal gas with con-

stant opacity (e.g., Kippenhahn et al. 2013). Most of the He and carbon core burning happens within the hot S Doradus instability strip (S Dor, gray band in Fig. 2), where the star spends 1.9×10^5 years for model “mix” and 8.1×10^4 years for model “primordial”.

Afterwards, both evolve into the observationally forbidden region beyond the Humphrey-Davidson limit (HD, dotted gray line in Fig. 2, Humphreys & Davidson 1994). Model “mix” spends there its last ~ 3800 years, while owing to its lower luminosity, the model “primordial” only spends ~ 600 years beyond the HD limit.

While both the S Dor strip and the HD limit have been observationally determined at $Z \approx Z_{\odot}$, Davies et al. (2018) recently showed that the empirical HD limit is likely metallicity-independent. This might support the theoretical results of Jiang et al. (2018), who found that He-opacity is the likely driver of outbursts in luminous stars close to the HD limit and the S Dor strip. Overall, LBVs are known at the metallicity of the Small Magellanic Cloud (e.g, Szeifert et al. 1993), and observation of narrow-lined SNe (in particular their isolation relative to other explosions) might be compatible with LBV eruptions happening in more metal-poor parts of galaxies.

The location of our merger models on the HR diagram suggests they could be affected by envelope instabilities and severe mass loss. The noisiness of the curves is

caused by the numerical instabilities, possibly related to physical instabilities in the envelopes (see Sec. 4.1).

The top right panel of Fig. 2 shows the evolution of the central temperature and density. By construction, both merger models avoid the instability region (gray area) and proceed to CC avoiding pulses. Conversely, a $140 M_{\odot}$ single star model, hits repeatedly the PI (although off-center, Renzo et al. 2020a) resulting in large mass loss. The bottom right panel shows the averaged adiabatic index Γ_1 which stays above the dotted line indicating instability (e.g., Renzo et al. 2020a). Conversely, the averaged adiabatic index of the $140 M_{\odot}$ model drops significantly below $4/3$ repeatedly during PI pulses.

4.1. Estimates for the continuum-driven mass loss

Fig. 3 shows the temporal evolution of the ratio of the luminosity L to the Eddington luminosity

$$L_{\text{Edd}} = \frac{4\pi GMc}{\kappa}, \quad (2)$$

where G is the gravitational constant, M the total mass, and c the speed of light. Dashed lines only consider electron-scattering opacity $\kappa \simeq 0.2(1 + X(^1\text{H})) \text{ cm}^2 \text{ g}^{-1}$, while solid lines correspond to using the stellar surface² opacity in the calculation of the Eddington luminosity.

Both our merger models evolve with high Eddington ratios, and the more luminous and He-rich “mix” model reaches ~ 1 about a thousand years before CC. Again, this suggests that radiatively-driven eruptive mass loss might occur even at low metallicity (e.g., Smith 2014). Increasing Z has a large effect over the opacity κ , decreasing L_{Edd} and thus increasing the Eddington ratio. Not surprisingly, preliminary calculations at $Z = 0.02$ with our simple setup proved to be numerically unstable.

Fig. 4 shows the internal structure and opacity profile at two selected times for our models. Solid lines correspond to when the models reach an effective temperature $\log_{10}(T_{\text{eff}}/[\text{K}]) = 4.5$, roughly in the S Dor instability strip, while dashed lines show models at $\log_{10}(T_{\text{eff}}/[\text{K}]) = 4.2$, beyond the HD limit.

While our models have $Z = 2 \times 10^{-4} \simeq Z_{\odot}/100$, two opacity bumps are still evident at both times, one caused by partial recombination of iron (Fe) roughly at $\log_{10}(T/[\text{K}]) \simeq 5.3$, and one due to partial He recombination at $\log_{10}(T/[\text{K}]) \simeq 4.6$. The presence of these opacity bumps drives inefficient convection layers (shading and hatching in Fig. 4). The interplay between den-

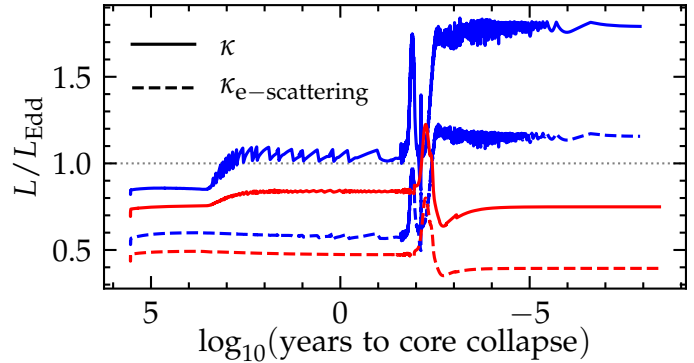


Figure 3. Eddington ratio post-merger as a function of the time left to CC. Solid lines use only the electron-scattering opacity for L_{Edd} , while the dashed lines use the total opacity. The blue (red) lines correspond to the “mix” (“primordial”) merger models. In both cases, the post-merger model exceeds Eddington ratio of 1 (dashed horizontal line), indicating that eruptive and/or continuum driven mass loss could occur.

sity inhomogeneities due to convection and the close-to-super-Eddington luminosity was found to be a key driver of LBV eruptions (at least at $Z = Z_{\odot}$, Jiang et al. 2015, 2018).

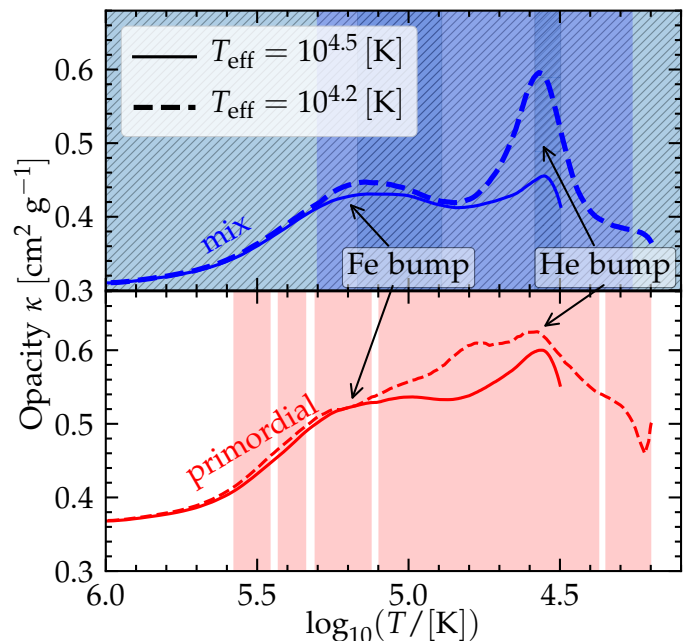


Figure 4. Outer structure of the opacity for two different values of the effective temperature. The top (bottom) panel shows the “mix” (“primordial”) model. The hatched regions indicate convection at $\log_{10}(T_{\text{eff}}/[\text{K}]) = 4.5$, with two separate regions in the “mix” model (and none in the “primordial” model). Colored regions mark convective regions at $\log_{10}(T_{\text{eff}}/[\text{K}]) = 4.2$.

² The surface opacity is the average of the Rosseland mean opacity from optical depth $\tau = 2/3$ down to $\tau = 100$.

Because of the as-yet insufficient theoretical understanding, our models do not include eruptive LBV-like mass loss or continuum-driven winds in addition to line-driven winds. Nevertheless, following Paxton et al. (2011); Cantiello et al. (2020) we can estimate the extra mass loss of models exceeding the Eddington luminosity as

$$\dot{M}_{\text{Edd}} \simeq -\frac{L - L_{\text{Edd}}}{v_{\text{esc}}^2}, \quad (3)$$

where L and L_{Edd} are the luminosity and Eddington luminosity, and v_{esc} is the surface escape velocity. We only use this to estimate in post-process the amount of mass the star would have lost, and we neglect the structural reaction this may cause (Renzo et al. 2017).

Fig. 5 shows the mass-loss rate history (bottom panel) and cumulative mass lost (top panel) for our “mix” model. The wind mass-loss rate (in blue, Vink et al. 2001) removes mass earlier on but becomes subdominant a few hundred years before CC. Then, the Eddington-driven mass loss (green, Eq. 3) becomes dominant. The total mass loss (thick purple) is the sum of the two and is only about $\sim 1 M_{\odot}$, corresponding to a total final mass of $\sim 98 M_{\odot}$. At higher Z more mass loss would be expected. The lower luminosity and Eddington ratio of the “primordial” model result in a smaller mass loss estimate than for the “mix” model.

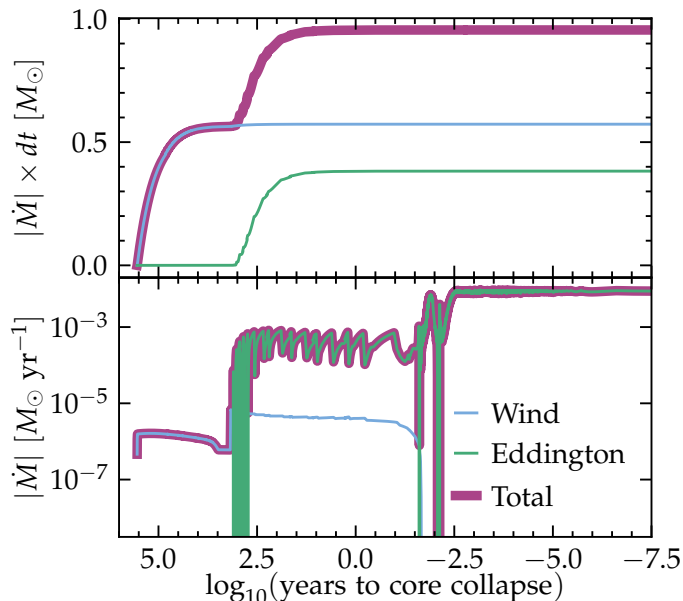


Figure 5. Absolute value of the mass loss rate (bottom) and cumulative mass loss (top) as a function of time until CC for our “mix” model.

5. DISCUSSION & CONCLUSIONS

We tested a stellar merger scenario for the production of BHs in the pair-instability mass gap. To avoid the pair-instability regime, this scenario assumes that the core mass of the primary star is unaffected by the merger, with the mass of the secondary fully mixed into the envelope (Spera et al. 2019; Di Carlo et al. 2019, 2020a,b). We do not explore how realistic this assumption is, which needs to be addressed using hydrodynamic calculations (e.g., Lombardi et al. 2002; Glebbeek et al. 2013; Schneider et al. 2019). Standard entropy-sorting post-merger structures would result in adding the He cores together, which would violate the hypothesis allowing these mergers to avoid the PPI regime.

Assuming the core does not grow, the envelope of the merger necessarily becomes He-enriched, with the extent of the enrichment depending on when the merger occurs during the main sequence of the secondary star. It could be prevented by allowing the least massive star in the merger to be younger (and less evolved) than the most massive one (e.g., our “primordial” model), so that less He is present in its core. Given the small lifetime differences between very massive stars, this would require not only a non-starburst star formation history, but also fine-tuned timing.

We use detailed stellar evolution calculations to evolve two merger products that assume either an evolved or an unevolved secondary. Because of the He-enrichment, the merger product can be significantly more luminous than a star of similar mass (cf. Fig. 2). It is already possible most stars with $M \gtrsim 100 M_{\odot}$ will experience large outbursts of mass loss (e.g., Conti 1975), and the He-richness might exacerbate this (Jiang et al. 2018). This suggests LBV-like outbursts or continuum driven mass-loss can occur even at metallicity as low as $Z = 2 \times 10^{-4} \simeq Z_{\odot}/100$.

We estimated the amount of mass that can be lost by these stellar merger products due to their proximity to the Eddington limit, and found that they can shed up to $\approx 1 M_{\odot}$ during the last few hundred years prior to core collapse (Sec. 4.1). This circumstellar material could leave visible imprints in the light curves and spectra of a terminal transient (e.g., Arcavi et al. 2017; Vigna-Gómez et al. 2019), if the final BH formation ejects (a small amount of) mass (e.g., Gilkis & Soker 2014; Quataert et al. 2019).

However, the amount of material lost during the evolution is not large enough to affect the scenario for BH formation in the pair-instability mass gap. We note that stronger mass loss is expected in more metal-rich environment, so that this scenario can only occur below a metallicity threshold. Ultimately, multidimensional ra-

diation hydro-dynamical simulations and a better theoretical understanding of LBV eruptions is needed to precisely quantify the pre-collapse mass of these luminous, He-rich merger remnants.

Finally an estimate of neutrino-driven mass loss (Nadezhin 1980; Lovegrove & Woosley 2013) is required to establish the actual size of the BH formed at core collapse. The oversized envelopes and He-enrichment keep our merger models relatively blue at the onset of core-collapse ($\log_{10}(T_{\text{eff}}/[\text{K}]) \gtrsim 4.1$), that is in the intermediate regime where the amount of mass loss at BH formation is unclear (e.g., Fernández et al. 2018). Further studies of the hydrodynamics at merger and at BH formation are needed to assess whether the “stellar merger

scenario” can contribute a significant populations of BHs inside the PISN mass gap.

In the meantime, population synthesis simulations could bracket the range of possibility by considering varying degrees of envelope mass loss before and at core-collapse.

Software: `mesaPlot` (Farmer 2018), `mesaSDK` (Townsend 2019), `ipython/jupyter` (Pérez & Granger 2007), `matplotlib` (Hunter 2007), `NumPy` (van der Walt et al. 2011), `MESA` (Paxton et al. 2011, 2013, 2015, 2018, 2019)

ACKNOWLEDGEMENTS

We are thankful to U. N. di Carlo, R. Fernandez, Y. Götzberg, Y. Levin, and N. Smith for helpful exchanges, and to the referee for the prompt and constructive feedback.

APPENDIX

A. MESA SETUP

We use MESA version 12778 to compute our models. The MESA equation of state (EOS) is a blend of the OPAL Rogers & Nayfonov (2002), SCVH Saumon et al. (1995), PTEH Pols et al. (1995), HELM Timmes & Swesty (2000), and PC Potekhin & Chabrier (2010) EOSes.

Radiative opacities are primarily from OPAL (Iglesias & Rogers 1993, 1996), with low-temperature data from Ferguson et al. (2005) and the high-temperature, Compton-scattering dominated regime by Buchler & Yueh (1976). Electron conduction opacities are from Cassisi et al. (2007).

Nuclear reaction rates are a combination of rates from NACRE (Angulo et al. 1999), JINA REACLIB (Cyburt et al. 2010), plus additional tabulated weak reaction rates Fuller et al. (1985); Oda et al. (1994); Langanke & Martínez-Pinedo (2000). Screening is included via the prescription of Chugunov et al. (2007). Thermal neutrino loss rates are from Itoh et al. (1996). We compute the pre-merger evolution using an 8-isotope α -chain nuclear reaction network and switch to a 22-isotope nuclear network for the post-merger evolution.

We evolve our models from the pre-main sequence to the terminal age main sequence of the most massive $58 M_{\odot}$ star, defined as the time when the central hydrogen abundance $X(^1\text{H}) \leq 10^{-4}$. We treat convection using the Ledoux criterion, and include thermohaline mixing (until the central temperature $\log_{10}(T_c/[\text{K}]) > 9.45$, Farmer et al. 2016) and semiconvection, both with an efficiency factor of 1. We assume $\alpha_{\text{MLT}} = 2.0$ and use Brott et al. (2011) overshooting for the convective core burning. We have tested that varying core overshooting does not impact significantly the post-merger evolution, however, when including shell overshooting and/or undershooting we were unable to find solutions to the stellar structure equations. Moreover, we employ the MLT++ artificial enhancement of the convective flux (e.g., Paxton et al. 2015; Jiang et al. 2015). Stellar winds are included using the algorithms from Vink et al. (2001) with an efficiency factor of 1.

To compute through the very late phases, we reduce the core resolution and increase the numerical solver tolerance when the central temperature increases above $\log_{10}(T_c/[\text{K}]) > 9.45$. We define the onset of core-collapse when the iron-core infall velocity exceeds 1000 km s^{-1} (e.g., Woosley et al. 2002).

The inlists, processing scripts, and model output will be made available at <https://zenodo.org/record/4062493>.

REFERENCES

- Abbott, R., Abbott, T. D., Abraham, S., et al. 2020a, arXiv e-prints, arXiv:2009.01075.
<https://arxiv.org/abs/2009.01075>
- . 2020b, arXiv e-prints, arXiv:2009.01190.
<https://arxiv.org/abs/2009.01190>

- Aghakhanloo, M., Murphy, J. W., Smith, N., & Hložek, R. 2017, *MNRAS*, 472, 591, doi: [10.1093/mnras/stx2050](https://doi.org/10.1093/mnras/stx2050)
- Angulo, C., Arnould, M., Rayet, M., et al. 1999, *Nuclear Physics A*, 656, 3, doi: [10.1016/S0375-9474\(99\)00030-5](https://doi.org/10.1016/S0375-9474(99)00030-5)
- Arcavi, I., Howell, D. A., Kasen, D., et al. 2017, *Nature*, 551, 210, doi: [10.1038/nature24030](https://doi.org/10.1038/nature24030)
- Barkat, Z., Rakavy, G., & Sack, N. 1967, *Physical Review Letters*, 18, 379, doi: [10.1103/PhysRevLett.18.379](https://doi.org/10.1103/PhysRevLett.18.379)
- Bartos, I., Kocsis, B., Haiman, Z., & Márka, S. 2017, *ApJ*, 835, 165, doi: [10.3847/1538-4357/835/2/165](https://doi.org/10.3847/1538-4357/835/2/165)
- Belczynski, K. 2020, arXiv e-prints, arXiv:2009.13526. <https://arxiv.org/abs/2009.13526>
- Belczynski, K., Hirschi, R., Kaiser, E. A., et al. 2020, *ApJ*, 890, 113, doi: [10.3847/1538-4357/ab6d77](https://doi.org/10.3847/1538-4357/ab6d77)
- Brott, I., de Mink, S. E., Cantiello, M., et al. 2011, *A&A*, 530, A115, doi: [10.1051/0004-6361/201016113](https://doi.org/10.1051/0004-6361/201016113)
- Buchler, J. R., & Yueh, W. R. 1976, *ApJ*, 210, 440, doi: [10.1086/154847](https://doi.org/10.1086/154847)
- Cantiello, M., Jermyn, A. S., & Lin, D. N. C. 2020, arXiv e-prints, arXiv:2009.03936. <https://arxiv.org/abs/2009.03936>
- Cassisi, S., Potekhin, A. Y., Pietrinferni, A., Catelan, M., & Salaris, M. 2007, *ApJ*, 661, 1094, doi: [10.1086/516819](https://doi.org/10.1086/516819)
- Chugunov, A. I., Dewitt, H. E., & Yakovlev, D. G. 2007, *PhRvD*, 76, 025028, doi: [10.1103/PhysRevD.76.025028](https://doi.org/10.1103/PhysRevD.76.025028)
- Conti, P. S. 1975, *Memoires of the Societe Royale des Sciences de Liege*, 9, 193
- Croon, D., McDerrott, S. D., & Sakstein, J. 2020a, arXiv e-prints, arXiv:2007.07889. <https://arxiv.org/abs/2007.07889>
- . 2020b, arXiv e-prints, arXiv:2007.00650. <https://arxiv.org/abs/2007.00650>
- Cyburt, R. H., Amthor, A. M., Ferguson, R., et al. 2010, *ApJS*, 189, 240, doi: [10.1088/0067-0049/189/1/240](https://doi.org/10.1088/0067-0049/189/1/240)
- Davies, B., Crowther, P. A., & Beasor, E. R. 2018, *MNRAS*, 478, 3138, doi: [10.1093/mnras/sty1302](https://doi.org/10.1093/mnras/sty1302)
- De Luca, V., Desjacques, V., Franciolini, G., Pani, P., & Riotto, A. 2020, arXiv e-prints, arXiv:2009.01728. <https://arxiv.org/abs/2009.01728>
- de Mink, S. E., Langer, N., Izzard, R. G., Sana, H., & de Koter, A. 2013, *ApJ*, 764, 166
- Di Carlo, U. N., Giacobbo, N., Mapelli, M., et al. 2019, *MNRAS*, 487, 2947, doi: [10.1093/mnras/stz1453](https://doi.org/10.1093/mnras/stz1453)
- Di Carlo, U. N., Mapelli, M., Bouffanais, Y., et al. 2020a, *MNRAS*, 497, 1043, doi: [10.1093/mnras/staa1997](https://doi.org/10.1093/mnras/staa1997)
- Di Carlo, U. N., Mapelli, M., Giacobbo, N., et al. 2020b, *MNRAS*, 498, 495, doi: [10.1093/mnras/staa2286](https://doi.org/10.1093/mnras/staa2286)
- Farmer, R. 2018, *rjfarmer/mesaplot*, doi: [10.5281/zenodo.1441329](https://doi.org/10.5281/zenodo.1441329)
- Farmer, R., Fields, C. E., Petermann, I., et al. 2016, *ApJS*, 227, 22, doi: [10.3847/1538-4365/227/2/22](https://doi.org/10.3847/1538-4365/227/2/22)
- Farmer, R., Renzo, M., de Mink, S., Fishbach, M., & Justham, S. 2020, arXiv e-prints, arXiv:2006.06678. <https://arxiv.org/abs/2006.06678>
- Farmer, R., Renzo, M., de Mink, S. E., Marchant, P., & Justham, S. 2019, *ApJ*, 887, 53, doi: [10.3847/1538-4357/ab518b](https://doi.org/10.3847/1538-4357/ab518b)
- Farrell, E. J., Groh, J. H., Hirschi, R., et al. 2020, arXiv e-prints, arXiv:2009.06585. <https://arxiv.org/abs/2009.06585>
- Ferguson, J. W., Alexander, D. R., Allard, F., et al. 2005, *ApJ*, 623, 585, doi: [10.1086/428642](https://doi.org/10.1086/428642)
- Fernández, R., Quataert, E., Kashiyama, K., & Coughlin, E. R. 2018, *MNRAS*, 476, 2366, doi: [10.1093/mnras/sty306](https://doi.org/10.1093/mnras/sty306)
- Fishbach, M., & Holz, D. E. 2020, arXiv e-prints, arXiv:2009.05472. <https://arxiv.org/abs/2009.05472>
- Fragione, G., Grishin, E., Leigh, N. W. C., Perets, H. B., & Perna, R. 2019, *MNRAS*, 488, 47, doi: [10.1093/mnras/stz1651](https://doi.org/10.1093/mnras/stz1651)
- Fragione, G., Loeb, A., & Rasio, F. A. 2020, arXiv e-prints, arXiv:2009.05065. <https://arxiv.org/abs/2009.05065>
- Fuller, G. M., Fowler, W. A., & Newman, M. J. 1985, *ApJ*, 293, 1, doi: [10.1086/163208](https://doi.org/10.1086/163208)
- Gaburov, E., Lombardi, J. C., & Portegies Zwart, S. 2008, *MNRAS*, 383, L5, doi: [10.1111/j.1745-3933.2007.00399.x](https://doi.org/10.1111/j.1745-3933.2007.00399.x)
- Gilkis, A., & Soker, N. 2014, *MNRAS*, 439, 4011, doi: [10.1093/mnras/stu257](https://doi.org/10.1093/mnras/stu257)
- Glebbeek, E., Gaburov, E., Portegies Zwart, S., & Pols, O. R. 2013, *MNRAS*, 434, 3497, doi: [10.1093/mnras/stt1268](https://doi.org/10.1093/mnras/stt1268)
- Heger, A., Langer, N., & Woosley, S. E. 2000, *ApJ*, 528, 368
- Humphreys, R. M., & Davidson, K. 1994, *PASP*, 106, 1025, doi: [10.1086/133478](https://doi.org/10.1086/133478)
- Hunter, J. D. 2007, *Computing In Science & Engineering*, 9, 90
- Iglesias, C. A., & Rogers, F. J. 1993, *ApJ*, 412, 752, doi: [10.1086/172958](https://doi.org/10.1086/172958)
- . 1996, *ApJ*, 464, 943, doi: [10.1086/177381](https://doi.org/10.1086/177381)
- Itoh, N., Hayashi, H., Nishikawa, A., & Kohyama, Y. 1996, *ApJS*, 102, 411, doi: [10.1086/192264](https://doi.org/10.1086/192264)
- Jiang, Y.-F., Cantiello, M., Bildsten, L., Quataert, E., & Blaes, O. 2015, *ApJ*, 813, 74, doi: [10.1088/0004-637X/813/1/74](https://doi.org/10.1088/0004-637X/813/1/74)
- Jiang, Y.-F., Cantiello, M., Bildsten, L., et al. 2018, *Nature*, 561, 498, doi: [10.1038/s41586-018-0525-0](https://doi.org/10.1038/s41586-018-0525-0)
- Justham, S., Podsiadlowski, P., & Vink, J. S. 2014, *ApJ*, 796, 121, doi: [10.1088/0004-637X/796/2/121](https://doi.org/10.1088/0004-637X/796/2/121)

- Kinugawa, T., Nakamura, T., & Nakano, H. 2020, arXiv e-prints, arXiv:2009.06922.
<https://arxiv.org/abs/2009.06922>
- Kippenhahn, R., Weigert, A., & Weiss, A. 2013, *Stellar Structure and Evolution* (Springer-Verlag), doi: 10.1007/978-3-642-30304-3
- Kremer, K., Spera, M., Becker, D., et al. 2020, arXiv e-prints, arXiv:2006.10771.
<https://arxiv.org/abs/2006.10771>
- Langanke, K., & Martínez-Pinedo, G. 2000, *Nuclear Physics A*, 673, 481, doi: 10.1016/S0375-9474(00)00131-7
- Langer, N. 1998, *A&A*, 329, 551
- Leung, S.-C., Nomoto, K., & Blinnikov, S. 2019, *ApJ*, 887, 72, doi: 10.3847/1538-4357/ab4fe5
- Lombardi, James C., J., Warren, J. S., Rasio, F. A., Sills, A., & Warren, A. R. 2002, *ApJ*, 568, 939, doi: 10.1086/339060
- Lovegrove, E., & Woosley, S. E. 2013, *ApJ*, 769, 109.
<https://arxiv.org/abs/1303.5055>
- Maeder, A., & Meynet, G. 2000, *ARA&A*, 38, 143, doi: 10.1146/annurev.astro.38.1.143
- Mapelli, M., Santoliquido, F., Bouffanais, Y., et al. 2020, arXiv e-prints, arXiv:2007.15022.
<https://arxiv.org/abs/2007.15022>
- Marchant, P., & Moriya, T. J. 2020, *A&A*, 640, L18, doi: 10.1051/0004-6361/202038902
- Marchant, P., Renzo, M., Farmer, R., et al. 2019, *ApJ*, 882, 36, doi: 10.3847/1538-4357/ab3426
- McKernan, B., Ford, K. E. S., Kocsis, B., Lyra, W., & Winter, L. M. 2014, *MNRAS*, 441, 900, doi: 10.1093/mnras/stu553
- McKernan, B., Ford, K. E. S., Lyra, W., & Perets, H. B. 2012, *MNRAS*, 425, 460, doi: 10.1111/j.1365-2966.2012.21486.x
- Menon, A., & Heger, A. 2017, *MNRAS*, 469, 4649.
<https://arxiv.org/abs/1703.04918>
- Morozova, V., Piro, A. L., Renzo, M., et al. 2015, *ApJ*, 814, 63, doi: 10.1088/0004-637X/814/1/63
- Nadezhin, D. K. 1980, *Ap&SS*, 69, 115, doi: 10.1007/BF00638971
- Oda, T., Hino, M., Muto, K., Takahara, M., & Sato, K. 1994, *Atomic Data and Nuclear Data Tables*, 56, 231, doi: 10.1006/adnd.1994.1007
- Paxton, B., Bildsten, L., Dotter, A., et al. 2011, *ApJS*, 192, 3, doi: 10.1088/0067-0049/192/1/3
- Paxton, B., Cantiello, M., Arras, P., et al. 2013, *ApJS*, 208, 4, doi: 10.1088/0067-0049/208/1/4
- Paxton, B., Marchant, P., Schwab, J., et al. 2015, *ApJS*, 220, 15, doi: 10.1088/0067-0049/220/1/15
- Paxton, B., Schwab, J., Bauer, E. B., et al. 2018, *ApJS*, 234, 34, doi: 10.3847/1538-4365/aaa5a8
- Paxton, B., Smolec, R., Schwab, J., et al. 2019, *ApJS*, 243, 10, doi: 10.3847/1538-4365/ab2241
- Pérez, F., & Granger, B. E. 2007, *Computing in Science & Engineering*, 9, 21
- Perna, R., Lazzati, D., & Cantiello, M. 2018, *ApJ*, 859, 48, doi: 10.3847/1538-4357/aabcc1
- Perna, R., Wang, Y.-H., Farr, W. M., Leigh, N., & Cantiello, M. 2019, *ApJL*, 878, L1, doi: 10.3847/2041-8213/ab2336
- Podsiadlowski, P. 1992, *PASP*, 104, 717, doi: 10.1086/133043
- Pols, O. R., Tout, C. A., Eggleton, P. P., & Han, Z. 1995, *MNRAS*, 274, 964, doi: 10.1093/mnras/274.3.964
- Potekhin, A. Y., & Chabrier, G. 2010, *Contributions to Plasma Physics*, 50, 82, doi: 10.1002/ctpp.201010017
- Quataert, E., Lecoanet, D., & Coughlin, E. R. 2019, *MNRAS*, 485, L83, doi: 10.1093/mnrasl/slz031
- Renzo, M., Farmer, R., Justham, S., et al. 2020a, *A&A*, 640, A56, doi: 10.1051/0004-6361/202037710
- Renzo, M., Farmer, R. J., Justham, S., et al. 2020b, *MNRAS*, 493, 4333, doi: 10.1093/mnras/staa549
- Renzo, M., Ott, C. D., Shore, S. N., & de Mink, S. E. 2017, *A&A*, 603, A118, doi: 10.1051/0004-6361/201730698
- Rodriguez, C. L., Kremer, K., Grudić, M. Y., et al. 2020, *ApJL*, 896, L10, doi: 10.3847/2041-8213/ab961d
- Rogers, F. J., & Nayfonov, A. 2002, *ApJ*, 576, 1064, doi: 10.1086/341894
- Roupas, Z., & Kazanas, D. 2019, *A&A*, 621, L1, doi: 10.1051/0004-6361/201834609
- Safarzadeh, M., & Haiman, Z. 2020, arXiv e-prints, arXiv:2009.09320. <https://arxiv.org/abs/2009.09320>
- Sakstein, J., Croon, D., McDermott, S. D., Straight, M. C., & Baxter, E. J. 2020, arXiv e-prints, arXiv:2009.01213.
<https://arxiv.org/abs/2009.01213>
- Saumon, D., Chabrier, G., & van Horn, H. M. 1995, *ApJS*, 99, 713, doi: 10.1086/192204
- Schneider, F. R. N., Ohlmann, S. T., Podsiadlowski, P., et al. 2019, *Nature*, 574, 211, doi: 10.1038/s41586-019-1621-5
- Smith, N. 2014, *ARA&A*, 52, 487, doi: 10.1146/annurev-astro-081913-040025
- Spera, M., Mapelli, M., Giacobbo, N., et al. 2019, *MNRAS*, 485, 889, doi: 10.1093/mnras/stz359
- Stone, N. C., Metzger, B. D., & Haiman, Z. 2017, *MNRAS*, 464, 946, doi: 10.1093/mnras/stw2260
- Szeifert, T., Stahl, O., Wolf, B., et al. 1993, *A&A*, 280, 508
- Timmes, F. X., & Swesty, F. D. 2000, *ApJS*, 126, 501, doi: 10.1086/313304

- Townsend, R. 2019, MESA SDK for Linux: 20190911,
doi: [10.5281/zenodo.2603170](https://doi.org/10.5281/zenodo.2603170)
- van der Walt, S., Colbert, S. C., & Varoquaux, G. 2011,
Computing in Science Engineering, 13, 22,
doi: [10.1109/MCSE.2011.37](https://doi.org/10.1109/MCSE.2011.37)
- van Son, L. A. C., De Mink, S. E., Broekgaarden, F. S.,
et al. 2020, ApJ, 897, 100,
doi: [10.3847/1538-4357/ab9809](https://doi.org/10.3847/1538-4357/ab9809)
- Vigna-Gómez, A., Justham, S., Mandel, I., de Mink, S. E.,
& Podsiadlowski, P. 2019, ApJL, 876, L29,
doi: [10.3847/2041-8213/ab1bdf](https://doi.org/10.3847/2041-8213/ab1bdf)
- Vink, J. S., de Koter, A., & Lamers, H. J. G. L. M. 2001,
A&A, 369, 574, doi: [10.1051/0004-6361:20010127](https://doi.org/10.1051/0004-6361:20010127)
- Woosley, S. E. 2017, ApJ, 836, 244,
doi: [10.3847/1538-4357/836/2/244](https://doi.org/10.3847/1538-4357/836/2/244)
- Woosley, S. E., Heger, A., & Weaver, T. A. 2002, Rev.
Mod. Phys., 74, 1015, doi: [10.1103/RevModPhys.74.1015](https://doi.org/10.1103/RevModPhys.74.1015)
- Zhao, X., & Fuller, J. 2020, MNRAS, 495, 249,
doi: [10.1093/mnras/staa1097](https://doi.org/10.1093/mnras/staa1097)